Analysis of Ly α absorption lines in the vicinity of QSOs

R. Srianand

Inter University centre for Astronomy and Astrophysics

Post bag 4, Ganeshkhind, Pune 411007, India

and

Pushpa Khare

Department of Physics, Utkal University, Bhubaneswar-751004, India

email: anand@iucaa.ernet.in and pk@utkal.ernet.in

(To appear in MNRAS)

Abstract

We have compiled, from the literature, a sample of Ly α forest lines in the spectra of 69 QSOs, all observed with a resolution between 60 to 100 km s^{-1}. The sample is studied for proximity effect. We have tried to account for the effect of blending which is inherent in the intermediate resolution sample, by calculating the column density distribution, using an effective velocity dispersion parameter, from the observed equivalent width distribution. The use of this column density distribution in the proximity effect analysis reduces the background intensity values by a factor of 2 to 3 compared to the values obtained by using the column density distribution obtained from high resolution observations. Evidence is presented for a weak correlation between the effective velocity dispersion parameter and equivalent width. Such a correlation if present can increase the background values by a factor of up to 1.5. Considerations of proximity in the spectra of 16 QSOs, from our sample, exhibiting damped Ly α lines gives a background intensity which is 3 times smaller than the values obtained from the whole sample, confirming the presence of

dust in the damped Ly α systems. Lines close to the QSOs are shown to be marginally stronger and broader compared to lines away from the QSOs. The Ly α lines with absorption redshift larger than emission redshift are shown to be uncorrelated with QSO luminosity, radio loudness or optical spectral index. These lines occur more frequently at high redshifts. Their presence is correlated weakly with the presence of associated metal line systems. The possibilities that the QSO emission redshift is considerably higher and that either the Ly α clouds or the QSOs have peculiar velocities are considered. It is argued that a combination of both these phenomenon may be required to account for the presence of these lines

Key words: QSO: absorption lines: Ly α: Proximity effect

1. INTRODUCTION

An inverse trend in the distribution of Ly α forest lines near the QSOs was first reported by Carswell et al. (1988) and was later confirmed by various groups. Using non parametric Q-Test Murdoch et al. (1986; here after MHPB), and Lu et al.(1991) showed that fewer lines, than the number predicted by the best fit power law redshift distribution, are present in the regions close to the QSOs. This was interpreted as being due to the increased ionization of Ly α clouds near the QSOs due to their radiation field, and was used, first by Bajtlik et al.(1988; here after BDO), to obtain the intensity of background UV radiation field.

Recently Bechtold (1994) with an extended sample of intermediate resolution, FWHM$\simeq 1\mathring{A}$, spectra showed that proximity effect is present near QSOs at very high significance level. The background intensity values obtained by her are consistent with earlier results, and are higher than the values expected from the QSOs and other AGNs.

Intermediate resolution samples of Ly α lines consist of large number of QSO sight lines and sample the redshift space more or less uniformly. These are thus free from the effects induced by peculiar distribution of lines along one or two QSO sight lines. However due to high number density of Ly α lines, the lines observed with intermediate resolution are usually blends and may lead us to wrong interpretations. In this paper we try to study

the effect of various sources of uncertainties in the background intensity calculations based on proximity effect. For this purpose we have collected intermediate resolution spectra of large number of QSOs, with similar S/N, from the literature. The details of the data used are given in section 2. In section 3 we study the general properties of lines with $z_{abs} < z_{em}$. In section 4, we discuss the proximity effect and the effect of curve of growth and the low resolution on the calculations of background intensity. The properties of lines close to the emission redshift are discussed in section 5. In section 6 we discuss the Ly α lines with $z_{abs} > z_{em}$. We consider two possible origins for these lines, and for each of these hypothesis we calculate the background intensity. Conclusions are presented in section 7.

2. DATA SAMPLE

Useful information regarding the QSOs used in our sample along with the references are given in Table 1. Emission redshift of the QSOs quoted in the literature are given as z_{em}. However it is known that most of these emission line redshifts are obtained from high ionization lines and may not represent the systemic redshifts. Tytler and Fan (1992) have given formulae to obtain the systemic redshifts. We have used these, with all available emission lines, to obtain the average values of corrected redshifts, z^c_{em} which are also given in Table 1. z_{min} is the larger of the observed minimum and the redshift corresponding to the Ly β emission. z_{max} is the maximum observable redshift for Ly α lines. Since in this paper we also study the Ly α lines with $z_{abs} > z^c_{em}$ Ly α lines, hereafter NVLs(negative velocity lines), the maximum limit is taken as z_{max} rather than z^c_{em}. E is the minimum detectable equivalent width of a line at 5 σ level in each spectra. In most of the cases these values are taken as given by of the authors of the parent references. Wherever these are not given we have taken E to be five times the largest observable error in the equivalent width of any line in the relevant redshift range. f_ν is the QSO continuum flux at the Lyman limit. The values are calculated by extrapolating the continuum flux at the rest wavelength of $\lambda(1450)$ to the Lyman limit. The spectral index α is also given in the Table. For QSOs for which the value of α is not available we use $\alpha = 0.66$. RL is the radio loudness, defined as

$$RL = \log\left(\frac{S(5GHz)}{S(\lambda 1450)}\right).$$

Wherever 5 GHz radio measurements are not available the radio flux was extrapolated from the other available radio measurements, assuming a powerlaw with 0.3 as the spectral index. Note that our sample has a large number of QSOs common with the sample compiled by Bechtold (1994). Out of 67 QSOs used here, 54 are from her sample. All the known metal lines and the Ly α belonging to metal line systems are considered as excluded regions. The Ly α lines with rest equivalent width $> 5\AA$ are also taken to be excluded regions as they may well be damped Ly α candidates.

3. REDSHIFT AND EQUIVALENT WIDTH DISTRIBUTION OF Ly α CLOUDS

In order to calculate the expected number of Ly α lines within the region near a QSO one should know the evolutionary properties of the lines with $z_{abs} < z_{em}$ without any ambiguity. Here we use our extended data to determine these properties. It is customary to describe the redshift and equivalent width distribution of Ly α lines as,

$$\frac{\partial^2 N}{\partial z \partial W} = A(1+z)^{\gamma} \exp \frac{-W}{W_*}, \qquad (1)$$

where $\frac{\partial^2 N}{\partial z \partial W}$ is the number of lines per unit redshift interval, per unit equivalent width, per line of sight. We used the maximum likelihood method described by MHPB, to calculate W_* and γ assuming them to be constant, independent of z and equivalent width, using the data described in the previous section. In order to have an unbiased sampling in the redshift space we confine ourselves to the redshift range between 1.7 to 3.7 and consider only those lines which are more than 8 Mpc (for $q_o = 0.5$) away from the QSO. The calculated values of γ for various rest equivalent width cutoffs, W_r^{min}, are given in table 2. Also given in table 2. are the values of KS probability that the largest difference between the observed redshift distribution and the distribution described by eqn (1), with the value of γ given by the fit, occurs by chance.

A glance at Table 2 reveals that there is a clear trend of increase in γ with an increase in w_r^{min}, consistent with Bechtold's result which is expected as 80% of the QSOs are in common

with her sample. As noted by her the γ values are lower than the previous estimates made with intermediate resolution observations. These are also somewhat lower than the estimates of γ made with high resolution sample (Srianand and Khare 1994; here after Paper I). The significance of the fit is very low for $W_r^{min} \leq 0.2\AA$ but is acceptable for higher values of W_r^{min}. This is primarily because, though the S/N of the spectra are good enough to detect even very weak lines, the poor resolution prevents us to deblend weak lines from the blended features. Low resolution thus introduces an incompleteness in the sample and also introduces a bias towards detecting weak lines more frequently at the lower redshifts, as the number density there is less than that at the higher redshift. This gives a smaller γ value, as well as produces an artificial differential evolution as was noticed by Liu & Jones (1988). The dependence of γ on W_r^{min} is however weaker, for $W_r^{min} \geq 0.25\AA$, than that found by Acharya and Khare (1993).Press, Rybicki and Schneider(1993), using a novel method, have obtained the value of γ to be 2.46$\pm$ 0.37. Their method makes use of the depression in the continuum on the short wavelength side of the Lyman alpha emission line and is free from any bias introduced due to the resolution used. Their data set is different and smaller compared to our data set. The difference between their value and the value obtained above is, however, not the effect of resolution as even the high resolution data (paper I) gives values smaller than their value.

The values of the equivalent width distribution parameter W_*, calculated using maximum likelihood method, for various W_r^{min} are also given in table 2. It is clear that unlike γ, W_* is independent of the rest equivalent width cutoff. As expected for the blended distribution, the values of W_* obtained here are higher than the corresponding values obtained from high resolution observations (Paper I).

We also performed two other statistical tests in order to estimate the goodness of fits. We used chi-square test to determine the χ^2 per degrees of freedom between the calculated and expected number of lines based on equation (1), using values of γ given by the fit, for individual QSOs. These values are also given in table 2. The χ^2 values indicate that the observed number of lines are not markedly different from the expected number in individual

QSOs. Also given in the table are the values of weighted average $< Q - 0.5 >$, as described by MHPB. Note that our values are nearly equal to zero, as one expects in the case where the assumed global distribution is consistent with the observed distribution in individual QSOs. In order to confirm this we performed Wilcoxon test described by Lu et al. (1991). Our results indicate that the probability that the observed values of $< Q - 0.5 >$ are distributed normally around zero, as is expected for a good fit, is 0.95 for $W_r^{min} = 0.3$Å. We define a parameter Y, $= n_e - n_o$, where n_e and n_o are the expected and observed number of lines in individual QSOs. If the distribution along individual sight lines is well described by the determined values of γ one expects Y to distribute normally around zero. The calculated probability for Y to be thus distributed, obtained using the Wilcoxon test, is 0.70 for $W_r^{min} = 0.3$Å. Therefore it is clear that redshift distribution of Ly α clouds described by the equation (1) is consistent with the observations if one considers lines which are more than 8 Mpc away from the QSOs.

4. PROXIMITY EFFECT

Tytler (1987) calculated the intensity of the intergalactic background (IGBR), $J_\nu = 10^{-21.7}$ ergs cm^{-2} s^{-1} Hz^{-1} Sr^{-1} at the Lyman limit based on QSO evolution studies, after accounting for absorption by intervening Lyman limit systems (LLS). He concluded that photoionization by QSOs alone can not explain the deficit of lines near the QSO unless the calculated background value has been over estimated by a factor ~ 60. BDO constructed the photoionization models of clouds near a QSO. Their model assumes the shape of the ionizing background radiation and that of the QSO continuum to be same. For a given cloud near QSO, the H I column density is given by

$$N_{H\,I} = N_o\,(1+\omega)^{-1}, \tag{2}$$

where N_o is what the column density would have been if there had been no nearby QSO and

$$\omega = \frac{F_\nu{}^Q}{4\pi J_\nu(z)}. \tag{3}$$

$J_\nu(z)$ is the IGBR at the Lyman limit, at redshift z, with which the clouds are in photoionization equilibrium and

$$F_\nu{}^Q = \frac{L_\nu}{4\pi {r_L}^2}, \tag{4}$$

is the local Lyman limit flux density due to the QSO, r_L being the luminosity distance of the cloud from the QSO. If the distribution of neutral hydrogen column density, $N_{H\,I}$ in individual clouds is a power law with index β, i.e. if

$$\frac{dN}{dN_{H\,I}} \propto {N_{H\,I}}^{-\beta} \tag{5}$$

then the number density of clouds above a column density threshold, N_o, is given by

$$N(N_{H\,I}) \propto {N_o}^{1-\beta}. \tag{6}$$

Hence, for a sample limited by lower column density $N_{H\,I}$, the distribution of lines with redshift in the spectra of a single QSO, including the proximity effect is

$$\frac{dN}{dz} \propto (1+z)^\gamma [(1+\omega(z))]^{1-\beta}. \tag{7}$$

BDO used $\beta = 1.7$, obtained from high resolution observations. They applied this equation to equivalent width limited samples assuming the following 3 idealizations. (1) the column density distribution, with $\beta = 1.7$ holds for clouds with column densities corresponding to equivalent widths greater than ${W_r}^{min}$. (2) column densities and velocity widths are uncorrelated (3) QSO proximity has no significant effect on velocity width. They obtained the IGBR to be, $J_\nu = 10^{-21.0\pm0.5}$ ergs cm^{-2} s^{-1} Hz^{-1} Sr^{-1} by fitting equation (7) to the observed data. Lu et al (1991), applying the same model to the extended low resolution data also got the same value of J_ν. Recently Bechtold obtained $J_\nu = 10^{-20.5}$ ergs cm^{-2} s^{-1} Hz^{-1} Sr^{-1} with her intermediate resolution data sample. Giallongo et al. (1993) based on column density limited sample consisting of 3 QSOs got the value of $J_\nu = 10^{-21.15}$ ergs cm^{-2} s^{-1} Hz^{-1} Sr^{-1}; they used $\beta = 1.53$ and $\gamma = 2.21$. This value of J_ν is less than the values obtained based on equivalent width limited samples, validity of which depends on the 3 assumptions made by BDO. Also this value is only two times larger than the value obtained from QSO number density evolution models. However results for high resolution sample consisting of 8 QSO spectra (paper 1) show that J_ν has to be higher than 10^{-21}.

Here we apply the models of BDO to our sample considering only the QSOs (marked by a * in Table 1.) which do not show LLS within 8 Mpc and do not show broad absorption lines. Any such line may shield the QSO radiation and may complicate the analysis of proximity effect. We used $\beta = 1.7$, $q_o = 1/2$, $W_r^{min} = 0.3$Å, and calculated the expected number of lines for various relative velocity bins near QSOs for various assumed values of J_ν. We used γ value obtained above. The value of J_ν obtained by minimizing χ^2 is $J_\nu = 10^{-20.22}$ ergs cm^{-2} s^{-1} Hz^{-1} Sr^{-1}. The probability that the predicted distribution, with best fit value of J_ν, represents the actual distribution is only 68%. For Bechtold's value of J_ν the probability falls to 61%. For the value of IGBR calculated by Madau (1992) the probability is as low as 10^{-6}. The value of of IGBR obtained here is much higher than the one expected from QSOs alone, and slightly higher than the previous estimates from proximity effects.

Due to proximity effect, the expected number n_e of Ly α lines near the QSOs, calculated from the general redshift distribution is expected to be more than their observed number n_o. Therefore $Y(= n_e - n_o)$, is expected to be distributed asymmetrically about zero. We have analysed this and have looked for the presence of any correlation between QSO properties with Y, for $W_r^{min} = 0.3$Å. One sample Wilcoxon test for lines within 8 Mpc and within r_{eq} (as defined by Tytler (1987)), which is the distance from the QSO at which the flux of radiation from QSO equals that due to the IGBR, for $J_\nu = 10^{-21}$ ergs cm^{-2} s^{-1} Hz^{-1} Sr^{-1} shows the probability for Y to be normally distributed around zero to be 0.49 and 0.44 respectively. We performed nonparametric Spearman rank correlation test in order to find any possible correlation between the properties of the QSO and Y. We do not find any correlation between Y and the properties of QSO such as, $z_{em}{}^c$, f_ν, α_o and RL.

It is interesting to note that there is no correlation between Y and f_ν. This is against our expectation if the proximity effect is induced by the excess ionization due to QSOs. Note that Lu et al.(1991) also do not find any correlation between luminosity, emission redshift or radio properties of the QSO and the proximity effect. Bechtold (1994) did not find proximity effect to depend on the radio properties or redshift but qualitatively found a dependence on

the luminosity of the QSOs.

Foltz et al. (1986) found an excess of C IV systems near the QSOs over that predicted by the distribution of C IV systems far from QSOs. The excess was shown to occur more frequently in the radio loud objects. These systems were attributed to absorption due to the galaxies in the cluster of which QSO is also a member. If the Ly α clouds are in some way associated with galaxies then there will be excess absorption near the QSO compared to that predicted by the general redshift distribution, more so for the radio loud QSOs. The lack of correlation between radio loudness and the proximity effect can not, however, be taken to indicate that there is no tendency of radio loud QSOs not to show associated Ly α absorption as we are not considering QSOs with LLS within 8 Mpc of the emission redshift. Thus in a way we tend to choose QSOs which are not having associated absorption and therefore are not residing in clusters.

4.1 Effect of uncertainties in column density distribution

The column density distribution of Ly α lines in individual cloud is not well determined due to the scarcity of high resolution data. Earlier studies by Carswell et al (1984) obtained that the value of $\beta \sim 1.7$. Recent analysis of Giallongo et al. (1993) showed that $\beta = 1.74$ fits the data with only 2% probability and for the lines with column density between $10^{13.2}$ and $10^{14.8}$ the best fit powerlaw is $\beta = 1.53$ with 70% probability. They also showed that the distribution is steeper for column density greater than $10^{14.8}$. In the case of 1331+170, Kulkarni et al (1994) obtained $\beta = 1.5$ for $13.1 < \log(N_{H\,I}) < 13.9$, and $\beta = 3.1$ for $13.9 < \log(N_{H\,I}) < 14.4$. In order to consider the effect of variation in β on the background intensity we varied the value of β and calculated χ^2 probability for various values of J_ν. The results are shown in fig 1. Also given in the figure are the expected values of the background intensity based on QSO counts for various forms of QSO evolution and intergalactic absorption (Madau 1992)

It is clear that the value of J_ν decreases with decrease in β, as has been earlier noted by Chernomordic and Ozernoy (1993); also the probability that the observed distribution is consistent with the predicted distribution increases. It is interesting to note that $\beta \sim$

1.2 – 1.3 will not only make the value of J_ν consistent with the one expected from QSO counts, but also will make the probability that the observed distribution is reproduced by the predicted distribution very high. Chernomordic and Ozernoy (1993) showed, using the analytic equation for curve of growth, that, in order to reproduce the observed equivalent width distribution the β value should be 1.4 rather than 1.7. In their calculations they assumed the value of velocity dispersion, b, to be 35 km s^{-1}, the mean value obtained from the high resolution observations. Assuming the b value of 25 km s^{-1} will reduce β below 1.3.

4.2 Effect of low resolution

The sample used for this analysis is obtained using low resolution spectra of QSOs. Most of the lines listed are actually blends of few narrow lines. In the case of metal line systems (Petitjean & Bergeron, 1990) the number of components is found to be correlated with the equivalent width of the blended line. Jenkins (1986) showed that large number of interstellar lines can be analysed collectively using the standard, single component curve of growth. As long as the equivalent widths of many line are combined and the distribution function for the line characteristics is not markedly irregular, one obtains nearly correct answer for the total column density even when different lines have large variation in their central optical depth and internal velocity dispersion. Also, the value of velocity dispersion, b, obtained from standard curve of growth of the blend will be higher than the one obtained by profile fitting of high resolution data and need not reflect any kinematic properties of the cloud, but is proportional to the number of clouds(Srianand & Khare, 1994). Thus one can write

$$N_{tot} = N_{tot}(1+\omega)^{-1}, \tag{8}$$

N_{tot} being the total column density of lines in the blend. Thus the form of the equation used by BDO is still valid, except that one has to use the distribution of total column density including blends, instead of the distribution of column density in individual components obtained from high resolution observations. Blending of lines in low resolution data may occur due to chance proximity of lines to each other but may also be enhanced due to

clustering of lines. Webb (1987) had found weak clustering among Ly α lines. Recently we (Paper I) also confirmed this from extended high resolution data. Barcons and Webb (1990) showed that the discrepancy between the column density distribution observed in high resolution data and that obtained from the equivalent width distribution at low resolution can not be accounted for by blending alone but can be explained by invoking clustering. This effect further invalidates the use of column density distribution obtained from high resolution data in the proximity effect calculations using low resolution data.

One can get the distribution of total column density, described by $\beta_{\rm LR}$, from the observed equivalent width distribution through standard single cloud curve of growth, with some assumed values of effective velocity dispersion, $b_{\rm eff}$. This is given by

$$f(N_{H\,I})dN_{H\,I} = f(W)\frac{dW}{dN_{H\,I}}dN_{H\,I} \qquad (9)$$

Assuming the standard forms for equivalent width and column density distribution one can get $\beta_{\rm LR}$ from W_* for a given value of $b_{\rm eff}$. We have determined $\beta_{\rm LR}$ from the observed equivalent width distribution of our sample for different values of $b_{\rm eff}$ restricting to the observed range of equivalent widths. $\beta_{\rm LR}$ values obtained for $W_* = 0.3\AA$ are given in table 3, with corresponding column density range obtained and the significance of the fit.

It is clear from that table that the value of $\beta_{\rm LR}$ decreases with the decrease in velocity dispersion. Though our Ly α sample contains strong lines, it does not contain Lyman limit clouds, which means the $N_{\rm tot} < 10^{17}$ cm s^{-2}. Note that blends of several clouds in a small velocity range ~ 200 km s^{-1} can produce a Lyman discontinuity if the total column density exceeds $\sim 2 \times 10^{17}$ cm s^{-2}. This condition ensures that the effective velocity dispersion of the blend is higher than 40 km s^{-1}. The high resolution profile fitted results show that the column density in individual clouds varies between $10^{13} - 10^{16}$cm^{-2}. Blending will effectively increase the column density cutoff values. Therefore the upper limit will be $\geq 10^{16}$cm^{-2}, and our $b_{\rm eff}$ should be able to produce this range of $N_{\rm tot}$. It can be seen from the table that in order to satisfy the above conditions the $b_{\rm eff}$ values should be between 40 and 50 km s^{-1}. Which means that the $\beta_{\rm LR}$ is between 1.4 -1.6.

One can in principle obtain the value of effective velocity dispersion using Ly α and Ly β lines and using doublet ratio method. This value, however, will be biased towards saturated lines, i.e. those which can produce measurable amount of Ly β. Hunstead et al.(1988) and Levshakov (1992) used Ly α and Ly β lines to calculate the effective column density of the blends. The observed column density range in these calculations is $10^{14.3} - 10^{16.8}$ with average velocity dispersion around 58 km s^{-1}, which is somewhat higher than the range obtained above. However the average value of equivalent width of Ly α lines used in their analysis is 0.78 $\AA$ which is higher than the average equivalent width , 0.58 $\AA$, in our sample. The lower equivalent width blends most likely have smaller b_{eff} unless they are formed due to blending of very large number of weak lines. Thus the range in velocity dispersion seems to be consistent with results of Hunstead et al(1986) and Levshakov (1992). Note that Press and Rybicki (1993) also found the value of β $\sim$1.4 from equivalent width ratios of Lyman series lines. Their value is independent of b. The equivalent width ratios were obtained by considering the depressions in the continuum, without resolving individual lines and are not biased.

Using β values in the range obtained here instead of β =1.7, the value of J_ν can at most be reduced by a factor of 2.5 (see fig 1.) but is still much higher than the value predicted from QSO counts alone.

The total equivalent width of a metal line like Mg II or C IV is known to be proportional to the number of components blended in the line (York et al. 1986; Petitjean & Bergeron 1990). Srianand and Khare (1994) showed that in order to explain the relationship between doublet ratio and W, for Mg II doublets, with single cloud curve of growth, one has to assume higher b values for lines with higher equivalent width. In paper I we showed that the column density distribution of lyman alpha lines in the blends is similar to the column density distribution of the rest of the lines. Thus strong lines are likely to have more components and we expect b_{eff} to increase with W. In addition there may also be an intrinsic tendency of b to increase with line strength for Lyman alpha lines (Pettini etal, 1990) though this has not not been confirmed by others (Carswell etal, 1991).If this kind of correlation exists in

the case of blended Ly α clouds it will affect our calculation of J_ν.

We used Hunstead et al.(1986) and Levshakov (1992) data to search for any such correlation. A clear correlation exists as shown in figure 2 and is described by,

$$b = 43.15 \times W + 31.38 \text{ km s}^{-1} \tag{10}$$

Taking into account this correlation,we again calculated β_{LR} for $W_* = 0.3$Å, with b_{eff} values given by the equation (10). β_{LR} was found to be, 1.87, which gives a background value higher than that estimated with $\beta_{LR} = 1.7$ by a factor of 1.5. Note that the above relation between W and b_{eff} is valid for high equivalent lines and may not necessarily hold for the whole range of W. However if valid, the correlation between b_{eff} and W will widen the difference between the values of J_ν calculated from proximity effect and from QSO counts.

4.3 Effect of dust obscuration due to intervening damped Ly α systems

A series of studies conducted by Fall and his collaborators (Fall, Pai & Mcmohan, 1989; Pai, Fall & Bechtold, 1991) indicate that the QSOs having intervening damped Ly α systems along the line of sight are redder than the rest of the QSOs. Recent studies by Pettini et al (1994), have confirmed the existence of dust in the damped Ly α systems. Though the fraction of dust to gas ratio is not as high as that in the case of the Milkyway, it does produce appreciable amount of reddening in the QSO spectra. The f_ν values calculated for these QSOs may thus be underestimates. IGBR calculations from proximity effect, considering only QSOs having damped Ly α absorbers are therefore expected to yield smaller values for the background radiation field compared to the values obtained using the whole sample. In order to check this, we considered only QSOs which show intervening damped Ly α systems and candidates (marked by d in Table 1) from our sample using the damped Ly α information given in Lanzetta et al (1991). There are 16 such QSOs in our sample. The value of J_ν is obtained to be 10^{-21} ergs cm^{-2} s^{-1} Hz^{-1} Sr^{-1}. This is smaller than the value obtained for the whole sample by a factor of 3. Our results thus confirm the reddening of QSOs due to intervening absorbers. This effect causes an error of upto a factor of 3 in the calculated J_ν values.

5. PHYSICAL PROPERTIES OF Ly α CLOUDS NEAR QSOs

In this section we search for any possible changes in physical properties of Ly α clouds like the equivalent width distribution, column density distribution, distribution of velocity dispersion and the distribution of expected and observed number of lines near the QSOs. Understanding how these properties change in the vicinity of the QSOs will yield a better understanding of the proximity effect.

5.1 Equivalent width distribution

We have calculated the equivalent width distribution of Ly α lines within 8 Mpc of the QSO for various values of W_r^{min}. The values of W_* are very similar to the values of W_* for lines away from the QSOs, given in table 2. KS test confirms that the two distributions are drawn from the same parent population. This is consistent with the results of earlier analysis (Sargent et al. 1980; Lu et al, 1991; Bechtold, 1994). However it is possible that the proximity effect does not extend to 8 Mpc and any change in the equivalent width distribution may show up if we restrict to regions within 'r_{eq}'. We have calculated the values of W_* for various values of w_r^{min} and of IGBR for lines within r_{eq} from the QSOs. The results are shown in figure 3. It is clear from the figure that the W_* increases for higher values of background intensity. This effect is more pronounced for the higher equivalent width lines. This suggests that the ratio of number of strong lines to that of weak lines increases near the QSO.

Assuming $J_\nu = 10^{-21}$ ergs cm^{-2} s^{-1} Hz^{-1} Sr^{-1} we calculated ω, the ratio of ionizing flux from the QSO and the background radiation flux, for each line within r_{eq}. Nonparametric Spearman rank correlation test was performed in order to find any correlation or anticorrelation between W and ω. No significant correlation was found for $W_r^{min} = 0.16$Å and 0.3Å. However there is 2.6σ correlation between the two quantities if we consider lines with equivalent width greater than 0.6Å. The null hypothesis that the two quantities are uncorrelated can be rejected at more than 99.6% confidence level. This again shows that strong lines tend to occur more frequently compared to weak lines near the QSOs. We thus conclude that the equivalent width distribution is affected by the excess photoionization due to QSO.

This may be due to increase in velocity dispersion in individual components or may be due to the effect of enhanced blending due to excess clustering of Ly α around the QSOs

5.2 Column density distribution

The change in the W_* near the QSOs suggests that the column density distribution may also be different in regions close to the QSOs. We therefore calculated the column density distribution of Ly α lines for various values of $N_{H\,I}^{min}$, considering lines within r_{eq} only for the high resolution data compiled in paper1, adding lines from Fan and Tytler (1994) for QSO 1946+7658. The results for various assumed values of J_ν are shown in figure 4. It can be seen from the figure that the error bars are too large to reveal any change in β. If any, there may be a slight decrease in β with increasing J_ν. Spearman rank correlation test between $N_{H\,I}$ and ω for $J_\nu = 10^{-21}$ ergs cm^{-2} s^{-1} Hz^{-1} Sr^{-1} for various $N_{H\,I}^{min}$ values does not show any significant correlation or anticorrelation between the two quantities. Therefore though figure 4 seems to indicate a slight decrease in β the rank correlation test does not show any statistically significant change in column density with ω which is consistent with the assumption of BDO that the column density distribution is unaltered by the presence of QSO.

5.3 Distribution of velocity dispersion parameter

The equivalent width and column density distributions near the QSOs suggest that the velocity dispersion parameter in clouds near QSOs may be higher. If the reported correlation between column density and b is true then also one would expect an increase in velocity dispersion due to proximity effect. Similar result is also expected on the basis of ionization models. In figure 6 we have plotted the distribution of b for clouds within 8 Mpc for $J_\nu = 10^{-21}$ ergs cm^{-2} s^{-1} Hz^{-1} Sr^{-1} for $\omega > 1$ and $\omega < 1$ separately. It is clear that low values of b, (i.e. b < 20 km s^{-1}) observed in $\sim 25\%$ of the cases for $\omega < 1$ are not seen in the case of $\omega > 1$. The clouds on an average have higher 'b' values when $\omega > 1$. Spearman rank correlation test between ω and b for $J_\nu = 10^{-21}$ ergs cm^{-2} s^{-1} Hz^{-1} Sr^{-1} shows 2.1σ correlation between ω and b. The null hypothesis that the two quantities are uncorrelated can be rejected at 96% confidence level. An increase in b will increase the b_{eff} and therefore

will give higher value for J_ν.

We thus conclude that the column density distribution seems to be similar for lines near as well as away from the QSO, while the velocity dispersion parameters and as a result the equivalent width distribution is different for the two classes of lines.

6. PROPERTITS OF NVLs

More than 50% of the QSO sight lines in our sample show narrow absorption features in the red wing of the Ly α emission which can not be attributed to any strong UV absorption belonging to previously known absorption systems listed by Junkkarinen et al.(1991). These are believed to be Ly α lines redshifted with respect to the QSO. Note that metal line systems with $z_{abs} > z_{em}$ have also been seen and are believed to be associated with the QSOs. They probably occur more frequently in radio loud or intrinsically faint QSOs (Foltz et al 1986; Moller & Jakobson, 1987).

In order to determine if the occurrence of the NVLs depends on any of the QSO properties, we first looked for the correlation between the presence of NVLs and the presence of associated metal lines, i.e. metal line systems within 8 Mpc of QSOs. Out of 15 QSOs not having NVLs only two show associated metal line absorption, whereas for 28 QSOs having at least one NVL 15 show metal line absorption within 8 Mpc. The occurrence of metal line systems near QSO and the occurrence NVLs thus seem to be correlated at about 7.5σ level. However we do not find any correlation between the number of associated metal line systems and the number of NVLs.

Next, we checked the possible correlation between the QSO flux at the Lyman limit, f_ν and the occurrence of NVLs. We did not find any correlation between these two quantities. There is no difference in the distribution of f_ν for QSOs which show NVLs and that for the rest of the QSOs.

The occurrence of NVLs also seems to be uncorrelated with the radio properties of QSOs. Out of 18 QSOs for which radio information is available, 2 radio quiet QSOs show more than 3 NVLs, 9 radio loud QSOs show more than one NVL and the rest 7 radio loud QSOs do not show any NVLs. We also do not find any correlation between optical spectral index , α

and the occurrence of NVLs. The distribution of optical spectral index for QSOs with and without NVLs are identical.

Next, we divided our sample into various redshift bins and calculated the ratio of the number of QSOs showing NVLs and the number of QSOs which do not show such lines, in each of these bins. The results are shown in figure 6. There is a clear increase in the ratio with redshift, implying that high redshift QSOs show NVLs more frequently than their low redshift counterparts. Also, there seems to be a weak trend of increasing number of NVLs in the spectra of an individual QSO with redshift of the QSO. The fraction of QSOs having a given number of NVLs is plotted in figure 7 for two different redshift bins.

In the framework of cosmological redshifts as distance indicators, we consider two possible origins for these lines, (1) The emission redshift of the QSOs used here may be wrong and may actually be higher than the values used here, (2) The redshifts are not the correct indicators of distance and peculiar velocities of the Ly α clouds or the QSOs can be the cause for NVLs Below we consider these possibilities and try to estimate the IGBR in each case.

6.1 Effect of emission line velocity shifts

In this section we consider the possibility that the observed Ly α lines with $z_{abs} > z^{c}_{em}$ are due to the underestimation of the QSO redshifts, and try to understand the results discussed in the previous section and the proximity effect in this scenario. Such a possibility has been considered by Espey (1993) who showed that a bias in the measurement of QSO redshifts can account for at least a portion of the discrepancy between the predicted values of the ionization background and the values resulting from the known QSOs. Note that the emission line redshifts used by us are obtained by using all observed emission lines and the analytic equations given by Tytler and Fan (1992). However these formulae assume a simple extrapolation of known results based on intermediate redshift QSOs, where both low as well as the high ionization lines are observable, to high redshifts, where most often the redshifts are based solely on the high ionization lines. Corbin (1990) showed that there is a clear correlation between v(Mg II - C IV), the velocity difference between the Mg II and C

IV emission lines, and absolute magnitude of the QSO. This was also confirmed by Tytler and Fan (1992). If Corbin relationship holds good for all redshifts then, due to the known luminosity evolution of QSOs (Boyle et al. 1988), the velocity shifts will be higher for higher redshift QSOs, and corrections applied by us may still be less than the actual offset values.

Following Espey (1993) we shifted all QSO redshifts by , v_s, and calculated the expected number for Ly_α lines in various relative velocity bins for $W_r^{min} = 0.3$Å. Espey (1993) considered only lines with z_{abs} less than the uncorrected emission redshift, z_{em} for the completeness of the sample. However as we have information beyond z_{em} for several QSOs, we consider all lines with z_{abs} less than the corrected emission redshift, z^s_{em}, after applying the shift, v_s. Inclusion of these lines will increase the size of the sample and should therefore give better (with smaller errors) values of the IGBR in this scenario.

The best fit values of J_ν obtained by minimizing χ^2, for various values of v_s and the probability for various values of v_s to describe the observations are given in Table 4. Increasing v_s decreases the value of IGBR however, the probability that the model reproduces the observations decreases. This is because large shifts predict more than the observed number of lines with $z^s_{em} < z_{abs} < z_{em}$. It thus appears that v_s has to be less than 1500 km s^{-1} in order to reproduce the observed distribution of Ly α clouds near the QSOs. There are, however, Ly α lines redshifted with respect to QSOs by more than 2500 km s^{-1}, which implies that at least in few QSOs the correction to the emission redshift may be much higher than the upper limit obtained from our analysis. Systemic corrections $\sim$ 5000 km s^{-1} have been obtained by Bechtold (1994) in few cases. In cases like 1331+170, however lines are seen upto a relative velocity of $\sim -10,000$ km s^{-1} (Kulkarni et al, 1994) and may require alternative explanation. The observed distribution of lines near the QSO and the distribution predicted for $v_s = 1000$ km s^{-1} is shown in figure 8 for $J_\nu = 10^{-21.0}$ ergs cm^{-2} s^{-1} Hz^{-1} Sr^{-1}

According to Corbin correlations we should expect large corrections to redshifts for more luminous objects and hence more number of NVLs, in these QSOs. However more luminous QSOs will also have stronger proximity effect, thereby reducing the number of such lines. The absence of any correlation or anticorrelation between the number of NVLs and f_ν or α

can thus be understood as the combined effect of Corbin correlations and proximity effect. Another trend found by us is that more number of NVLs tend to occur at high redshifts. This can be understood as an increase in the shift, v_s, with redshift for a constant background or an increase in IGBR with increasing redshift.

6.2 Effect of peculiar velocities

Another explanation for NVLs may be the presence of large peculiar velocities of the intervening Ly α clouds on top of the general Hubble flow. These peculiar velocities may either be due to the gravitation induced clustering of clouds associated with collapsed density peaks as in the models of Rees (1986) or due to the origin of clouds in the fragmenting shells as in the models proposed by Ostriker and Ikeuchi (1983). If Ly α clouds are formed in the extended galactic halos, in extended disks or in dwarf galaxies, one would expect them to have some peculiar velocity on top of the Hubble flow. It is also possible that QSOs themselves have peculiar velocities. In what follows we assume that all the Ly α clouds have peculiar velocities. We neglect the peculiar motions of QSOs keeping in mind that neglecting the peculiar velocities of Ly α clouds and considering peculiar motion of QSOs alone is identical to what is considered here as far as the proximity effect is concerned. The distribution of the line of sight component of the peculiar velocities of Ly α clouds is assumed to be gaussian given by,

$$f(v) = \frac{1}{\sqrt{\pi} v_d} \exp\left[- \left(\frac{v}{v_d} \right)^2 \right], \tag{11}$$

where v_d is the dispersion in peculiar velocity. Taking into account the I-model discussed by BDO, one can write the number of absorption lines expected at any redshift z along the line of sight to a QSO to be,

$$N(z) = \frac{N_o}{\sqrt{\pi} v_d} \int_0^{z_{em}^c} (1+z_1)^{\gamma+1} (1+\omega)^{1-\beta} \exp\left[- \frac{v(z,z_1)^2}{v_d^2} \right] dz_1, \tag{12}$$

where

$$\frac{v(z,z_1)}{c} = \frac{(1+z_1)^2 - (1+z)^2}{(1+z_1)^2 + (1+z)^2}, \tag{13}$$

c being the velocity of light in km s^{-1}. Taking the value of $\beta = 1.7$ and the value of γ obtained above we calculated the expected number of lines in bins with different relative velocities with respect to QSOs for various values of v_d and J_ν.

Considering only bins between -2500 and 6000 km s^{-1}, the χ^2 probability that the predicted number of lines is consistent with the observed values are given in Table 5. The expected distribution for $v_d = 2000$ km s^{-1} and $J_\nu = 10^{-20.5}$ergs cm^{-2} s^{-1} Hz^{-1} Sr^{-1} is shown in figure 8. It is clear from the table that J_ν has to be higher than $10^{-20.5}$ ergs cm^{-2} s^{-1} Hz^{-1} Sr^{-1} with v_d around 2000 km s^{-1} in order to fit the observed distribution. This value of peculiar velocity is very large. Dressler et al.'s (1987) analysis indicates that the peculiar velocities of galaxies are about 600 km s^{-1} relative to the microwave background. However the peculiar velocities of clusters of galaxies are around 2000 km s^{-1} (Bahcall, 1988).

If the high values of peculiar velocities are real then one would expect to get excess correlation upto the scale of few thousand km s^{-1} in the pair velocity correlation function of Ly α lines. However, studies conducted by various groups do not show any such excess beyond 300 km s^{-1}. It is possible that the NVLs may be Lyman alpha clouds associated with the galaxies in the cluster of galaxies containing the QSO. Presence of such a population of Lyman alpha clouds, distinct from the intergalactic Lyman alpha clouds, is indicated by the HST observations (Lanzetta etal 1995). This is also supported by the correlation of the NVLs and associated absorption systems, noted above. The peculiar velocities, in this case may be confined to this population of Lyman alpha clouds and may not, therefore, show up in the two point correlation of the entire population. However the peculiar velocities of galaxies in cluster are known to be only about 600 km s^{-1} as noted above and unless the peculiar velocities of the galaxies in the QSO containing cluster are larger than those in other clusters, it is unlikely that the NVLs are caused by the peculiar velocities alone. Also most of the associated metal line systems which are formed by galaxies in such clusters have metallicity close to or larger than the of solar value. If Ly α clouds are members of the QSO cluster then they are expected to be large in order to have detectable neutral hydrogen and

thus they would have accompanying high ionization metal lines. Such lines have not been observed. It thus seems unlikely that NVLs are produced by such absorbers. If these clouds are highly ionized massive clouds then one should frequently see x-ray absorption in such high z QSOs. Thus the x-ray observations of high z QSOs can be utilized to put bound on the fraction of lines that can be possibly present in the cluster containing the QSO.

One can consider the possibility that the QSOs themselves have peculiar velocities of ~ 2000 km s^{-1} on top of the Hubble flow. The values of J_ν and v_d obtained above will be valid for this case also. In order to have such a high velocity, QSO host clusters should have a mass of about $\sim 10^{16} M_\odot$ and more than 50 % of the QSOs should form in such massive cluster environments. The formation of such massive structures at redshifts as early as $z = 4$ is difficult in the currently favored models of structure formation. We can thus rule out the possibility that NVLs are produced due to peculiar velocities of Ly α clouds or those of QSOs. Also if this scenario was correct it will widen the discrepancy between the calculated background and that expected from the QSO counts alone.

It is clear from the above analysis that there is no unique mechanism by which one can explain the presence of NVLs. However a systemic offset of 1000-1500 km s^{-1} with a peculiar velocity dispersion of 500 km s^{-1} may explain the NVLs. The background intensity calculated in such a model will be similar to the values obtained by considering proximity effect for lines with $z_{abs} < z_e$ alone and the discrepancy between the background intensity calculated by using proximity effect and from QSO counts will persist.

7. CONCLUSIONS

A large sample of 69 QSOs,all observed with intermediate resolution between 60 and 100 km s^{-1} has been complied. The sample contains 1671 lines with equivalent width $> 0.3\AA$. It is analysed for evolutionary properties and proximity effect. The following conclusions are drawn.

(1) Ly α lines more than 8 Mpc away from QSOs give $W_* = 0.285 \pm 0.008$ and $\gamma = 1.725 \pm 0.228$.

(2) The analysis of proximity effect among Ly α lines close to the QSO, gives

$J_\nu = 10^{-20.22}$ ergs cm $^{-2}$ s^{-1}Hz^{-1} Sr^{-1}

(3) Value of J_ν obtained from proximity effect is shown to be sensitive to the assumed column density distribution and decreases by a factor of 3 if the powerlaw index of the distribution is changed from 1.7 to 1.4.

(4) It is proposed that the column density distribution, obtained from the observed equivalent width distribution assuming an effective velocity dispersion parameter should be used in the I-model calculations of the proximity effect in an intermediate resolution sample. This is shown to reduce the necessary background flux by a factor of 2.5.

(5) A correlation between the effective velocity dispersion parameter and equivalent width is shown to be likely to be present. Such a correlation, if present, tends to increase the background radiation flux.

(6) Considerations of proximity effect in the spectra of 16 QSOs, from our sample exhibiting damped Ly α lines, gives a background intensity 3 times smaller than the value obtained from the whole sample, confirming the presence of dust in the damped Ly α systems.

(7) The equivalent width distribution of Ly α lines close to QSOs is shown to be flatter than the distribution away from QSOs.

(8) The average velocity dispersion parameter for lines near the QSOs is shown to be higher by a factor of 1.2 than that for lines away from the QSOs.

(9) The occurrence of Ly α lines with absorption redshift larger than the emission redshift of the QSO is shown to be uncorrelated with QSO luminosity, optical spectral index or radio loudness. It is shown to be correlated with the redshift of the QSO as well as with the presence of associated metal systems.

(10) The number of absorption lines with redshift higher than the emission redshift in a QSO spectra is shown to increase with redshift.

(11) An underestimate of systemic redshift of QSOs by about 1500 km s^{-1} can explain the distribution of lines near QSOs including NVLs. However the significance of the fit is shown to decrease as one tries to fit the high velocity NVLs. Though this scenario reduces the IGBR by a factor of 2 to 3 it fails to explain the higher velocity NVLs.

(12) Very high peculiar velocities $\sim$ 2000 km s^{-1} of the Ly α clouds or the QSOs are needed to account for the occurrence of NVLs assuming no underestimate of systemic redshift. The required values of IGBR is higher than that obtained without peculiar velocities.

(13) Both the above effects namely higher systemic redshifts of the QSOs and peculiar velocities of Ly α clouds (or QSOs) together may explain the occurrence of NVLs.

In this work we have highlighted some of the issues that one has to consider while calculating the IGBR based on proximity effect. Understanding the origin of NVLs is very important as it plays a vital role in the calculations of IGBR. It can also provide some important clues towards our understanding of the QSO properties and the structures in the early universe. Only a large, column density limited, samples obtained by profile fitting of high resolution data can give a better estimation for the IGBR as the curve of growth effects seem to produce an uncertainty of about a factor of up to 5 in the calculated values of IGBR.

We wish to thank Dr. V. Sahani, Dr. K. Subramaniam and Dr. B. S. Sathyaprakash for useful discussions regarding peculiar velocities. This work was supported by a grant No. SP/S2/021/90 by the Department of Science and Technology, Govt. of India.

REFERENCES

[1] Bahcall, N. 1988, ARAA,26,631

[2] Bajtlik, S., Duncan, R. C., & Ostriker, J.P. 1988, Ap. J., 327 570 (BDO)

[3] Barcons, X., & Webb, J. R. 1990, MNRAS, 244,30p

[4] Bechtold, J. 1994, ApJS, 91, 1

[5] Boyle, B. J., Shanks, T., & Peterson, B. A. 1988, MNRAS, 238, 935

[6] Carswell, R. F., Lanzetta, K.M., Parnell, H. C., Webb, J. K. 1991, Ap.J.,371,76

[7] Carswell, R. F., Morton, D. C., Smith, M. G., Stokton, A. N., Turnshek, D. A., & Weymann, R. J. 1984, Ap. J, 278,486

[8] Carswell, R. F., Whelan, J. A. J., Smith, M. G., Boksenberg, A., & Tytler, D. 1982, MNRAS, 198, 91

[9] Chernomodic, V. V., & Ozernoy, L. M. 1993, Ap. J, 405, L5

[10] Corbin, M. R. 1990, Ap. J, 357, 346

[11] Dressler et al. 1987, Ap. J, 313, L37

[12] Espey, 1993, Ap. J, 411, L59

[13] Fall, S. M., Pai, Y. C., & McMohan, 1989, Ap. J, 341,L5

[14] Fan, X.,& Tytler, 1994, ApJS,

[15] Foltz, C. B., Weymann, R. F., Peterson, B. M., Sun, L., Malkan, M. A., & Chaffee, F. H. 1986, Ap.J., 307,504

[16] Giallongo, E., Cristiani, S., Fontana, A., & Travese, D. 1993, Ap. J., 416, 137

[17] Hunstead, R. W., Murdoch, H. S., Peterson, B., Blades, J. C., Jauncey, D. L., Wright, A. E., Pettini., & Savage, A. 1986, Ap. J, 304,496

[18] Jenkins, E. B. 1986, Ap. J, 322, 96

[19] Junkkarinen, V., Hewitt, A., & Burbidge, G. 1991, ApJS, 77,203

[20] Kulkarni, V. P., Welty, D., York, D. G., Huang, K. F, Green, R., & Bechtold, J. 1994 preprint

[21] Lanzetta, K. M., Wolfe, A. M., Turnshek, D. A., Lu, L., McMohan, G., & Hazard, C. 1991, ApJS,77,1

[22] Levshakov, S. A. 1992, AJ, 104, 950

[23] Liu. X. D., & Jones, B. J. T. 1988, MNRAS, 230, 481

[24] Lu, L., Wolfe, A. M., & Turnshek, D. A. 1991, Ap. J., 367,19

[25] Lu, L., Wolfe, A. M., Turnshek, D. A., & Lanzetta, K. M. 1993, ApJS, 84, 1

[26] Madau, P. 1992, Ap. J, 389, L1

[27] Moller, P.,& Jakobson, P. 1987, Ap. J, 320, L75

[28] Murdoch, H. S., Hunstead, R. W., Pettini, M., & Blades, J. C. 1986, Ap. J, 309, 19 (MHPB)

[29] Pai, Y. C., Fall, S. M., & Bechtold, J. 1991, Ap. J, 378, 6

[30] Petitjean, P., & Bergeron, J. 1990, A&A, 231, 309

[31] Pettini, M., Hunstead, R. W., Smith, L. J., Mar, D. P., 1990, MNRAS,246, 545

[32] Pettini, M., Smith, L. J., Hunstead, R. W., King, D. L. 1994, Ap. J,426,79

[33] Press, W. H., Rybicki, G. B. & Schneider, D. P. 1993, Ap. J,414,64

[34] Press, W. H.& Rybicki, G. B. 1993, Ap.J,418,585

[35] Sargent, W. L. W., Young, P. J.,& Boksenberg, A. 1982, Ap. J. 252,54

[36] Sargent, W. L. W., Young, P. J., Boksenberg, A., Carswell, R. F. & Whelan, J. A. J. 1979, Ap. J., 230,49

[37] Sargent, W. L. W., Boksenberg, A., & Steidel, C. C. 1988, ApJS, 68,539

[38] Sargent, W. L. W., Young, P. J., Boksenberg, A., & Tytler, D., 1980, ApJS, 42,41.

[39] Steidel, C. C. 1990a, ApJS, 72,1

[40] Steidel, C. C. 1990b, ApJS, 74,37

[41] Srianand, R., & Pushpa Khare, 1994, Ap. J, 428, 82

[42] Srianand, R., & Pushpa Khare, 1994, MNRAS, 271, 81 (paper1)

[43] Turnshek, D. A, Wolfe, A. M, Lanzetta, K. M., Briggs, F. H., Cohen, R. D., Foltz, C. B., Smith, H. E. & Wilkes, B. J. 1989, Ap. J., 344, 567

[44] Tytler, D. 1987, Ap. J, 321, 69

[45] Tytler, D., & Fan, X. 1992, ApJs, 79, 1

[46] Webb, J.K., Ph.D. thesis, Cambridge Univ., 1987

[47] Willinger, G. M., Carswell, R. F., Webb, J. K., Boksenberg A. & Smith, M. G. 1989, MNRAS, 237, 635

[48] Wolfe, A. M., Turnshek, D. A., Lanzetta, K. M., & Lu, L. 1993, Ap. J., 404, 480

[49] York, D. G., Dopita, M., Green, R., & Bechtold, J. 1986, Ap. J, 311, 610

[50] Young, P. J., Sargent, W. L. W. & Boksenberg, A. 1982, Ap. J., 252, 10

Figure Captions

Fig 1. χ^2 probability for various values of β and J_ν. Dotted line indicates the value of IGBR obtained by Madau (1992) based on QSO number density.

Fig 2. Velocity dispersion parameter for individual blends vs. equivalent width with the best fit line.

Fig 3. Equivalent width distribution parameter W_* for lines within r_{eq} vs. J_ν.

Fig 4. Column density distribution parameter β for lines within r_{eq} vs. J_ν.

Fig 5. Distribution of velocity dispersion for $\omega < 1$ and $\omega > 1$.

Fig 6. Ratio of number of QSOs with and without NVLs as a function of redshift.

Fig 7. Fraction of QSOs showing NVLs as a function of number of NVLs.

Fig 8. Histogram showing observed number of Ly α lines as a function of relative velocity with respect to QSO. Solid line shows the observed distribution. Dotted line shows the expected number for $v_s = 1000\,\mathrm{km\,s^{-2}}$ and $J_\nu = 10^{-21}\,\mathrm{ergs\,s^{-1}\,cm^{-2}\,st^{-1}\,Hz^{-1}}$. Dashed line shows the expected number for $v_d = 2000\,\mathrm{km\,s^{-2}}$ and $J_\nu = 10^{-20.5}\,\mathrm{ergs\,s^{-1}\,cm^{-2}\,st^{-1}\,Hz^{-1}}$.

TABLES

TABLE I. Data sample

QSO	z_{em}	$z_{em}{}^{c}$	z_{min}	z_{max}	E	f_{ν}^{+}	α	RL	ref.
0000-263*d	4.111	4.114	3.303	5.580	0.15	586	1.090	quiet	9
0001+087*	3.243	3.241	3.035	3.421	0.14	270	0.290	.....	1
0002+051*	1.899	1.900	1.764	2.628	0.16	663	1.010	2.00	2
0002-422*	2.763	2.767	2.175	3.418	0.30	301	.....	0.87	3,4
0014+813*	3.384	3.387	2.743	3.483	0.15	909	1.600	2.55	1
0029+073	3.294	3.262	2.869	3.384	0.14	377	1.070	....	1
0042-264*	3.298	3.300	3.192	5.950	0.15	337	.....	....	9
0055-269*d	3.653	3.663	3.347	5.909	0.15	177	0.470	....	9
0058+019*d	1.960	1.961	1.789	1.969	0.13	405	0.800	0.18	5
0114+089*	3.205	3.163	2.685	3.434	0.08	317	0.750	....	1
0142-100*	2.719	2.728	2.142	2.922	0.13	658	.....	0.60	5
0149+336*d	2.430	2.432	2.174	3.195	0.15	191	0.900	....	12
0201+365	2.912	.....	2.298	2.611	0.15	...	.....	. ....	11
0237-233*	2.222	2.225	1.756	3.121	0.13	844	0.170	2.51	5
0256-000*	3.374	3.377	2.685	3.434	0.18	408	0.580	....	1
0301-005	3.223	3.226	2.759	3.212	0.12	280	0.890	....	1
0302-003*	3.286	3.290	2.685	3.434	0.17	459	0.630	....	1,8
0334+204*d	3.126	3.312	3.043	3.212	0.06	227	0.650	....	1
0347-383*d	3.230	3.233	3.146	5.909	0.15	248	0.750	0.90	9
0421+019*	2.051	2.055	1.772	2.826	0.16	131	0.850	2.93	2
0424-131*	2.166	2.168	1.906	2.581	0.12	59	1.500	2.72	5
0428-136	3.244	.....	3.162	5.909	0.20	...	.....	....	9
0453-423*	2.656	2.657	2.209	3.402	0.32	323	.....	0.81	3,4
0636+680*	3.174	3.178	3.043	3.212	0.13	1382	1.200	3.52	1

0731+653*	3.033	3.038	2.677	3.359	0.30	160	0.660	2.58	1
0831+128*	2.739	2.737	2.156	2.825	0.29	161	0.660	....	1
0837-109*	3.326	3.329	2.989	3.442	0.10	178	.....	....	5
0848+163*	1.925	1.926	1.764	2.251	0.07	108	0.460	1.20	5
0905+151*	3.173	3.175	3.043	3.212	0.07	72	.....	....	1
0913+072*d	2.784	2.786	2.193	2.825	0.19	495	.....	....	1
0938+119*d	3.192	3.194	3.043	3.212	0.12	46	0.320	3.06	1
0953+549	2.584	2.586	2.018	2.574	0.15	350	.....	....	10
0956-122*	3.306	3.306	2.964	3.330	0.15	270	0.490	....	8
1017+280*d	1.928	1.929	1.632	2.661	0.10	1344	1.040	....	5
1017-106	3.158	3.158	2.855	3.222	....	...	.....	....	8
1033+137*	3.092	3.094	3.043	3.212	0.05	253	.....	loud	1
1115+080*	1.725	1.728	1.682	2.489	0.16	648	1.040	0.60	2
1151+068*d	2.762	2.764	2.173	3.216	0.30	130	0.900	....	7
1159+124*	3.502	3.504	2.795	3.607	0.20	881	0.220	....	5
1206+119	3.108	3.110	2.784	3.269	0.09	279	.....	....	1
1208+101*	3.822	3.825	3.400	4.018	0.11	333	1.260	....	1
1215+330*d	2.606	2.617	2.043	2.784	0.16	154	0.320	2.32	1
1225+317*	2.200	2.210	1.698	2.979	0.16	1169	0.620	2.20	4
1244+349*d	2.500	2.502	2.180	2.714	0.15	69	0.640	....	12
1247+267*d	2.039	2.042	1.680	2.455	0.08	573	0.620	0.60	5
1334+005	2.842	.....	2.242	2.783	0.07	560	.....	....	1
1400+114*	3.177	3.179	3.043	3.212	0.13	115	.....	....	1
1402+044	3.206	3.211	3.032	3.384	0.30	45	0.740	3.40	1
1409+093	2.912	.....	2.236	2.838	0.30	...	....	....	11
1410+096*	3.313	3.316	3.032	3.384	0.09	134	.....	....	1
1442+101*	3.554	3.535	2.872	3.582	0.09	278	0.380	3.38	1

1451+123	3.251	3.257	3.032	3.384	0.20	157	.....	....	1
1512+132*	3.120	3.122	2.872	3.228	0.25	64	.....	....	1
1548+092*d	2.748	2.749	2.455	2.907	0.29	336	.....	....	1
1601+182*	3.227	3.229	3.032	3.384	0.22	34	.....	....	1
1602+178*	2.989	2.991	2.749	3.105	0.40	32	1.220	....	1
1614+051*	3.216	3.217	3.032	3.384	0.25	22	.....	3.98	1
1623+269*	2.526	2.527	1.973	3.623	0.15	413	0.310	....	5
1738+350*	3.239	3.240	3.032	3.384	0.32	25	0.660	3.09	1
2000-330*	3.777	3.783	3.113	5.909	0.14	328	0.750	loud	9
2126-158*d	3.280	3.267	2.608	4.179	0.32	577	1.430	3.22	4
2204-408*	3.169	3.171	3.129	5.909	0.15	363	.....	....	6
2233+131*d	3.295	3.298	3.032	3.384	0.14	235	0.820	....	1
2233+136*	3.209	3.216	2.869	3.384	0.09	199	0.540	....	1
2239-386	3.511	.....	3.442	5.909	0.30	...	....	....	9
2311-036*	3.048	3.048	2.750	3.121	0.37	92	0.680	....	1
2359-022	2.810	.....	2.473	2.578	0.15	...	.....	....	12

ref: (1) Bechtold (1994), (2) Young, Sargent & Boksenberg (1982), (3) Sargent et al.(1979), (4) Sargent et al. (1980), (5) Sargent, Boksenberg & Steidel (1988), (6) Willinger et al. (1989), (7) Turnshek et al. (1989), (8) Steidel (1990b), (9) Steidel (1990a), (10) Levshakov (1992), (11) Lu et al. (1993), (12) Wolfe et al. (1993).

$*$ QSOs used for the proximity effect analysis

d QSOs which have intervening damped Ly α absorbers

$+$ f_ν is in units of microjanskies

TABLE II. Results of maximum likelihood analysis

W_r^{min}	γ	P_{KS}	W_*	χ^2	$< Q_K - 0.5 >$
0.16	1.0624±0.1944	1e-22	0.2858±0.0079	1.66	0.0043
0.20	1.4161±0.2015	1e-11	0.2824±0.0076	1.29	-0.0005
0.25	1.7553±0.2270	0.95	0.2780±0.0080	1.34	0.0043
0.30	1.7245±0.2279	0.57	0.2850±0.0080	0.92	-0.0005
0.45	2.2480±0.3016	0.66	0.2840±0.0100	1.47	0.0102
0.60	2.1730±0.3880	0.65	0.2780±0.0130	1.48	0.0132

TABLE III. Effective column density distribution

b_{eff}	range of N(H I)	β_{LR}	significance
30	14.2–18.0	1.1628	0.99
40	14.0–17.3	1.3769	0.99
50	14.0–16.2	1.6035	1.00
60	13.9–15.5	1.8343	1.00
70	13.9–14.8	2.0803	1.00

TABLE IV. Results of proximity effect calculations taking into account possible shift in systemic redshifts

v_s	$\log J_\nu^*$	χ^2 (prob)
0	-20.2	0.68
500	-20.6	0.97
1000	-21.0	0.91
1500	-21.4	0.86
2000	-21.6	0.61

$*$ J_ν is in units of ergs cm^{-2} s^{-1} Hz^{-1} Sr^{-1}

TABLE V. Results of proximity effect calculations taking into account the effect of peculiar velocities

	χ^2 probability for		
v(Km s^{-1})	$J_\nu^* = 10^{-20}$	$J_\nu^* = 10^{-20.5}$	$J_\nu^* = 10^{-21}$
1000	0.0000	0.0000	.....
1500	0.0036	0.1527	.....
2000	0.7468	0.6032	0.0009
2500	0.6578	0.5733	0.0096
3000	.....	0.5044	.....

$*$ J_ν is in units of ergs cm^{-2} s^{-1} Hz^{-1} Sr^{-1}

Fig 1

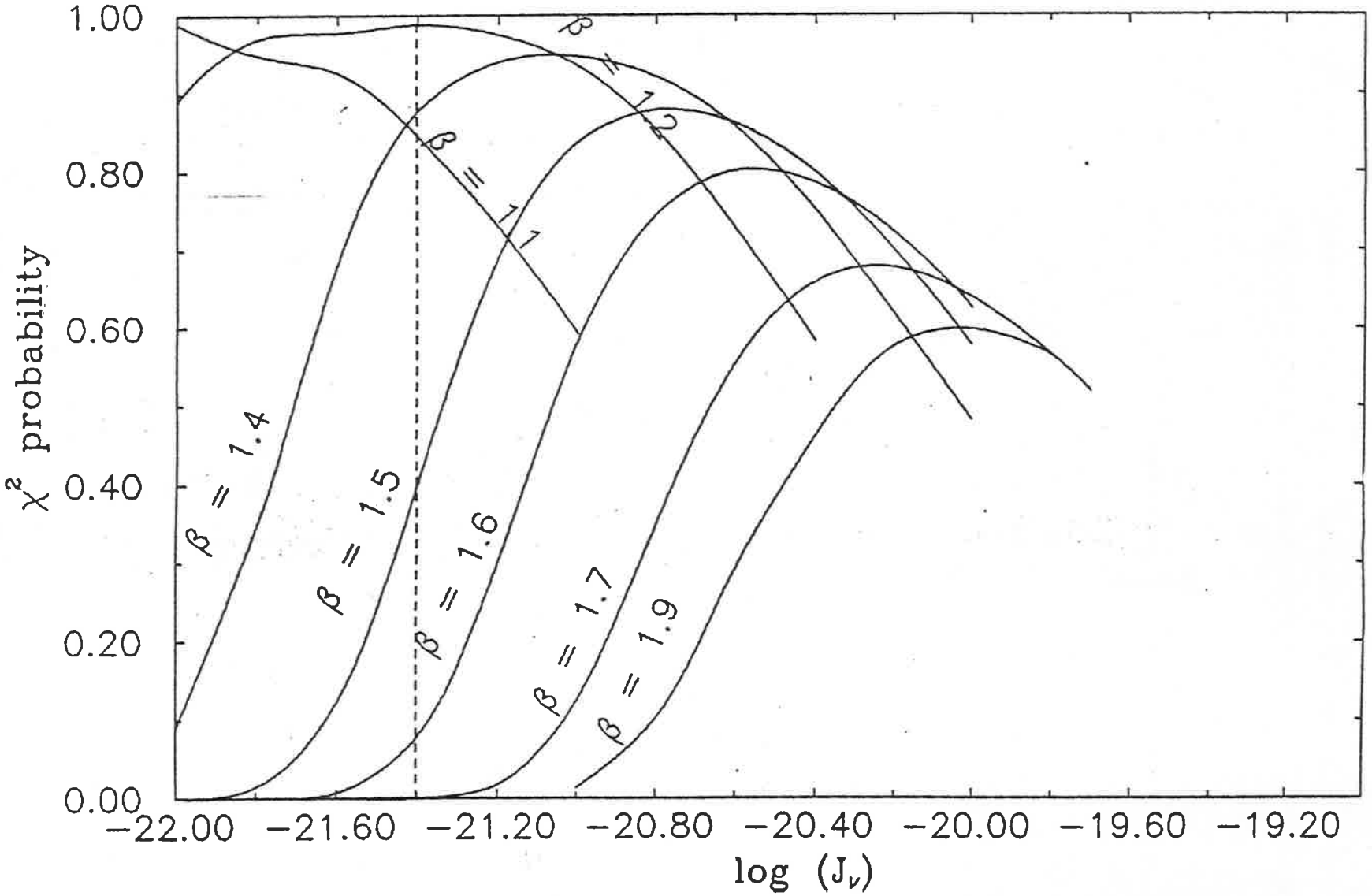
1.00
0.80
0.60
0.40
0.20
0.00
χ^2 probability
β = 1.4
β = 1.5
β = 1.6
β = 1.7
β = 1.9
β = 1.1
β = 1.2
−22.00
−21.60
−21.20
−20.80
−20.40
−20.00
−19.60
−19.20
log (J$_\nu$)

Fig 2

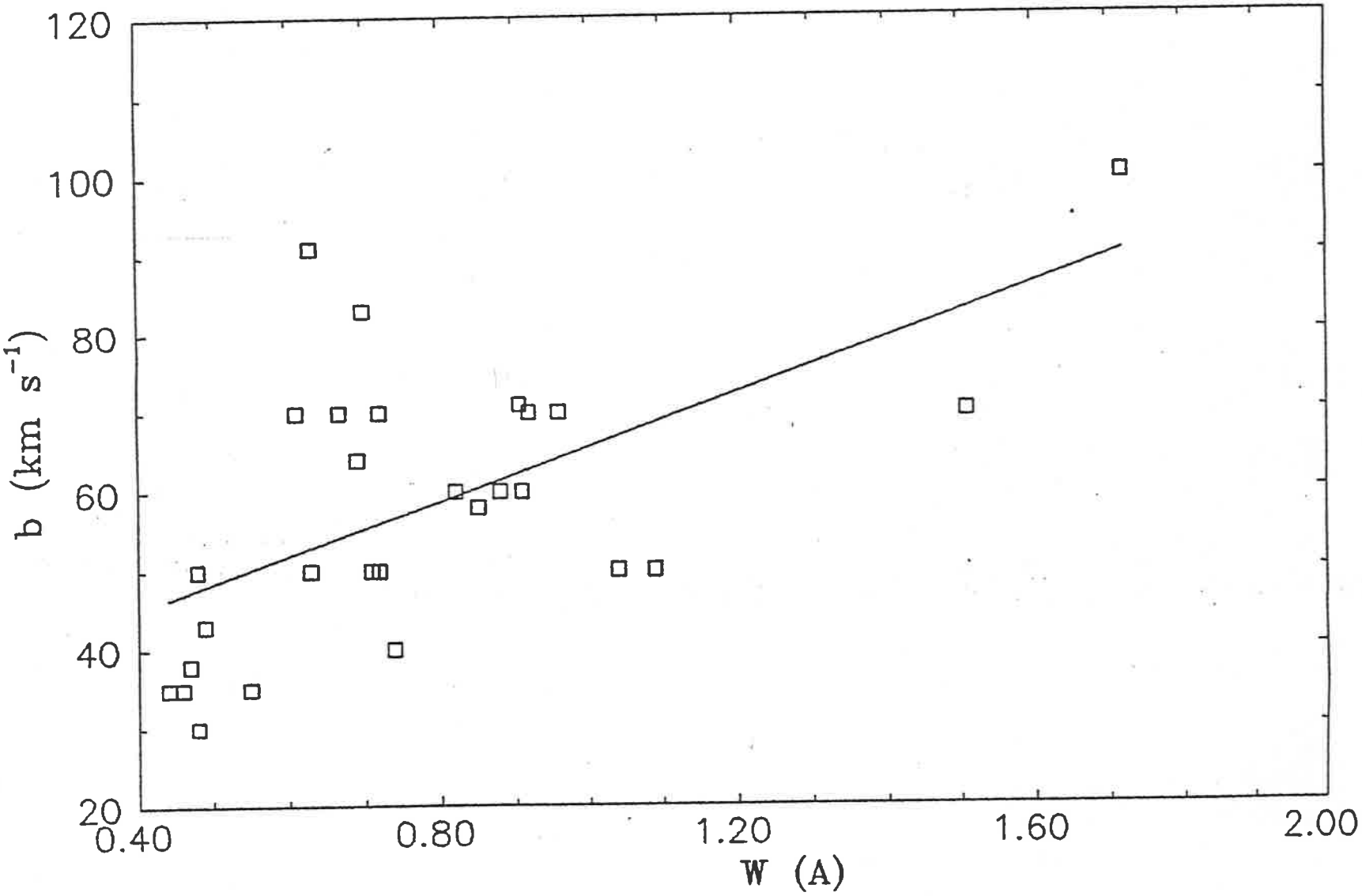

Fig 3

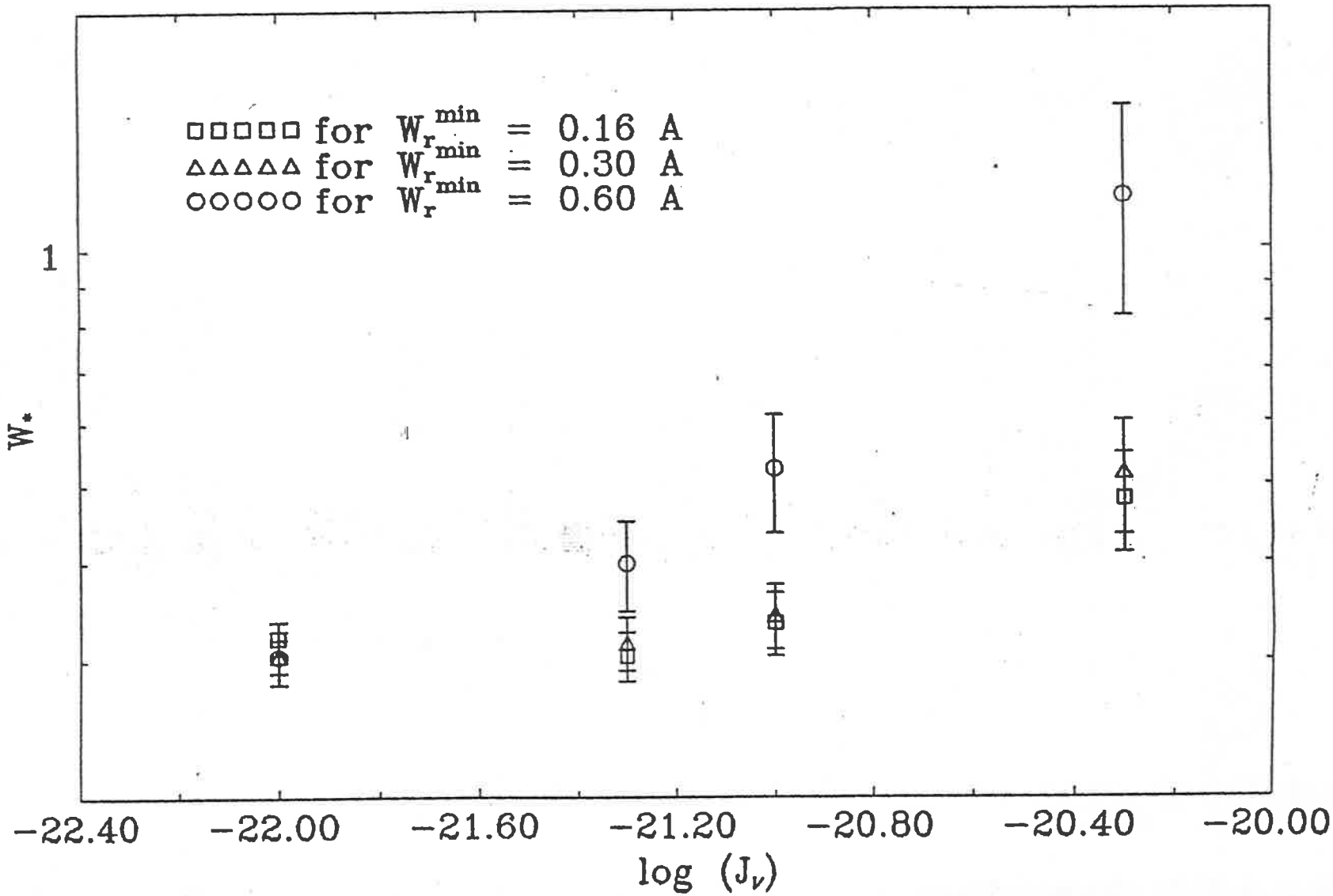
□□□□□ for $W_{r_{min}}$ = 0.16 A
△△△△△ for $W_{r_{min}}$ = 0.30 A
○○○○○ for $W_{r_{min}}$ = 0.60 A
1
W_*
−22.40
−22.00
−21.60
−21.20
−20.80
−20.40
−20.00
log (J_ν)

Fig 4

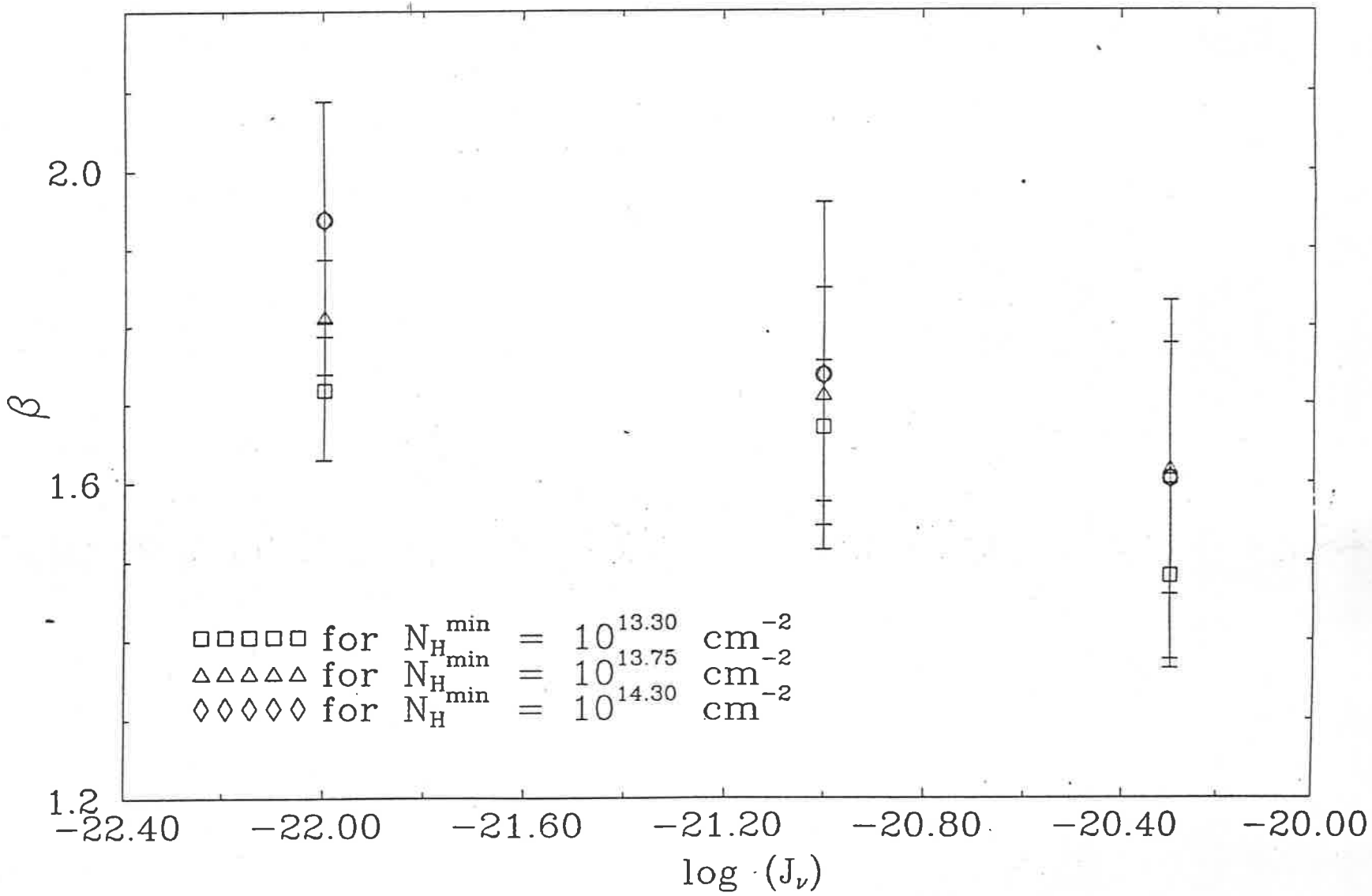
2.0
1.6
1.2
β
−22.40
−22.00
−21.60
−21.20
−20.80
−20.40
−20.00
log (J$_\nu$)
□□□□□ for $N_{H_{min}} = 10^{13.30}$ cm^{-2}
△△△△△ for $N_{H_{min}} = 10^{13.75}$ cm^{-2}
◊◊◊◊◊ for $N_{H_{min}} = 10^{14.30}$ cm^{-2}

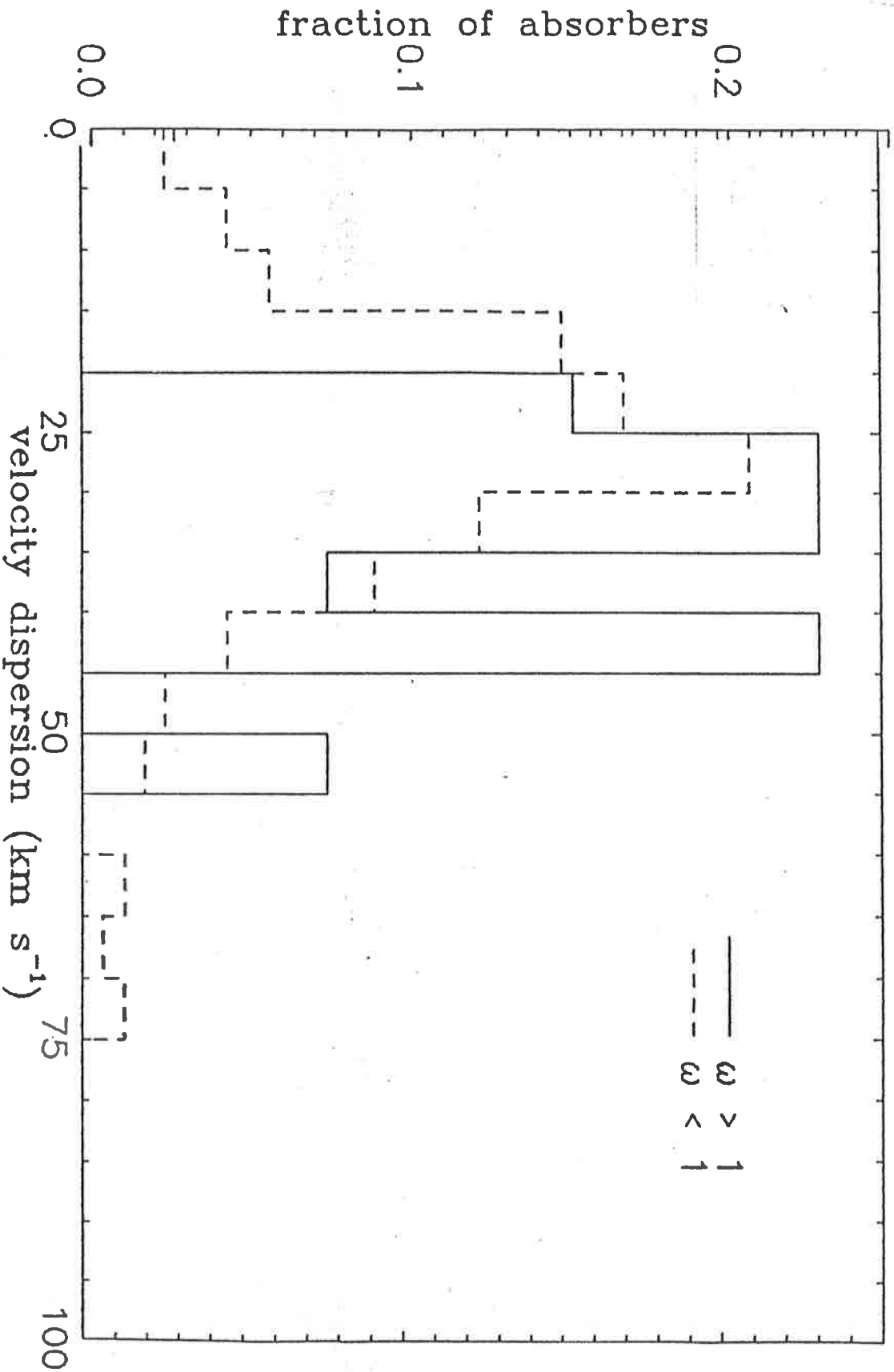
fraction of absorbers
0.0
0.1
0.2
0
25
50
75
100
velocity dispersion (km s^{-1})
$\omega > 1$
$\omega < 1$

Fig 5

Fig6

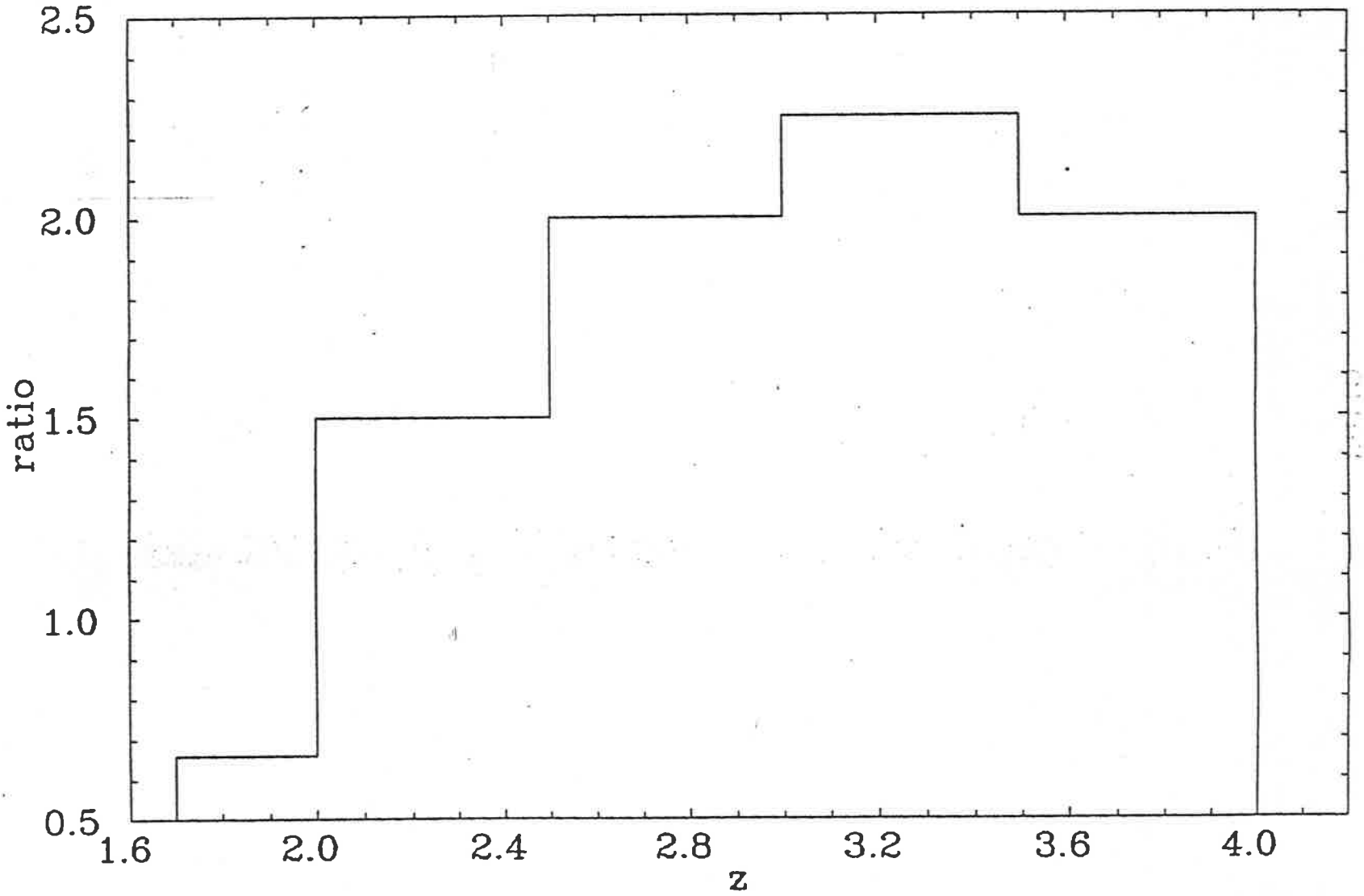

Fig 7

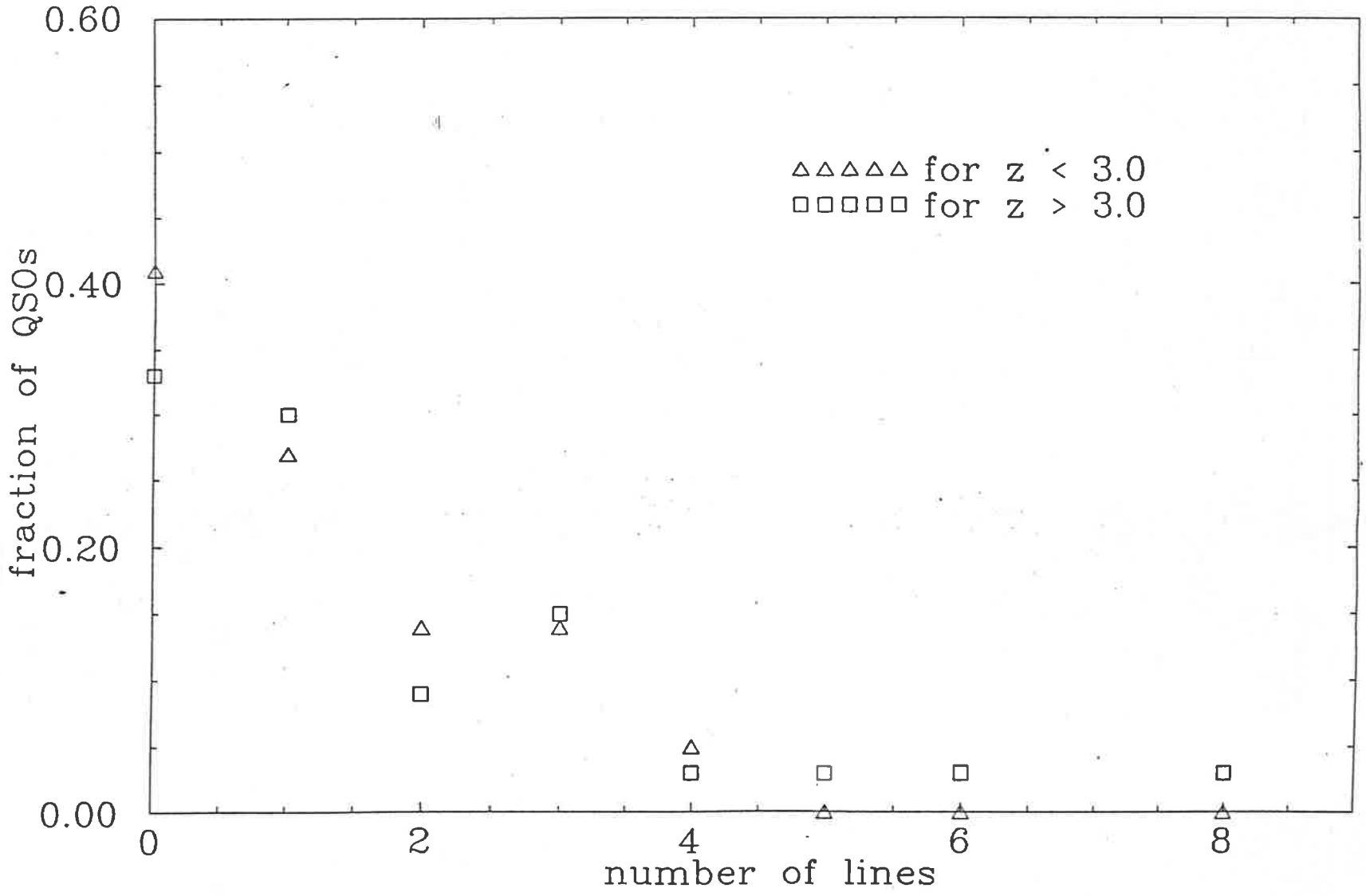
0.60
0.40
0.20
0.00
fraction of QSOs
△△△△△ for z < 3.0
□□□□□ for z > 3.0
0
2
4
6
8
number of lines

Fig 8

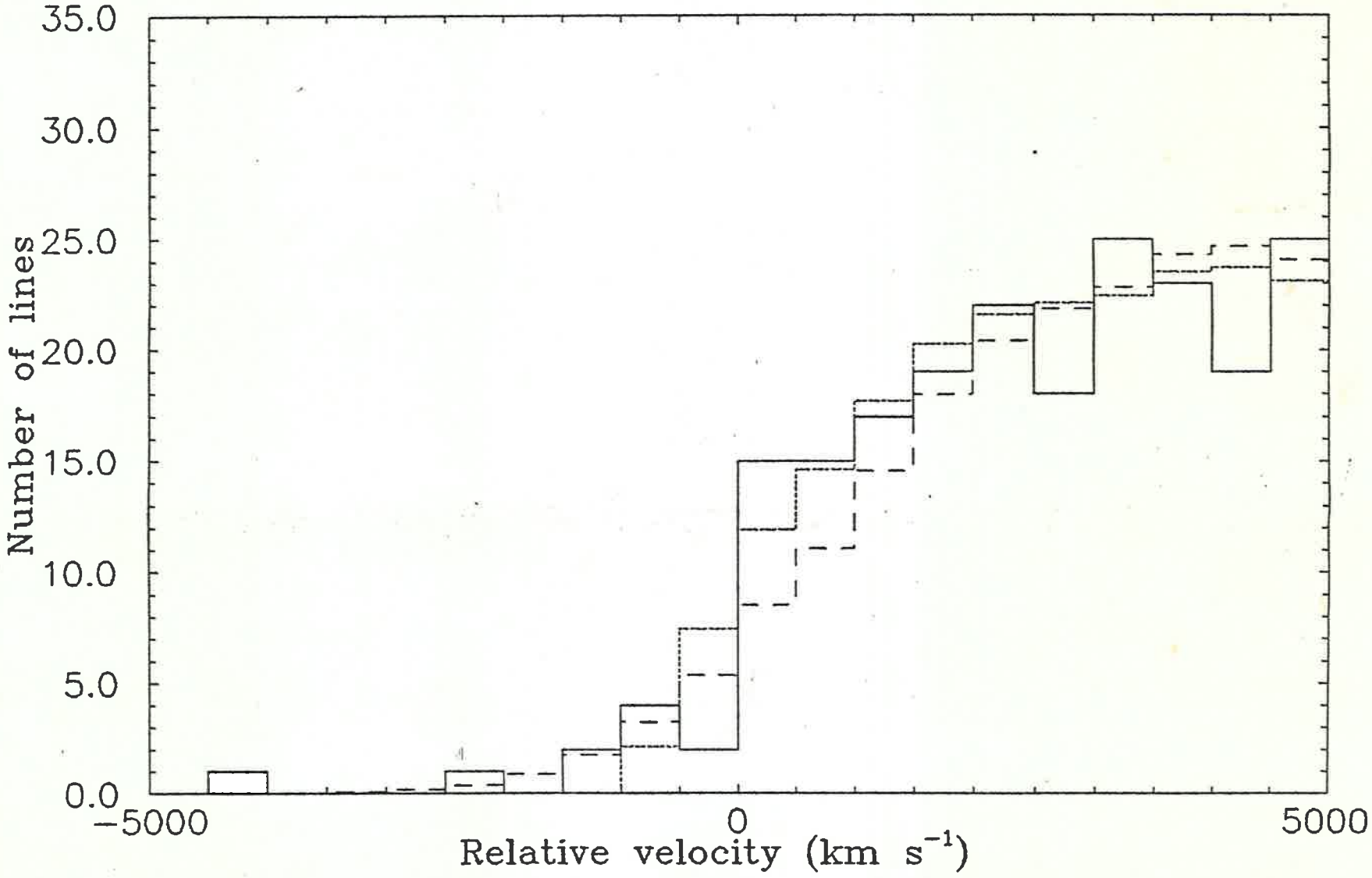
35.0
30.0
25.0
20.0
15.0
10.0
5.0
0.0
Number of lines
−5000
0
5000
Relative velocity (km s^{-1})